Adsorption mechanism of recovering potassium from seawater by modified-clinoptilolite using microwave

Hao Guo, Chang-Sheng Peng, Chang-Jiang Kou, Jian-Yun Jiang, Fan Zhang and He-Tao Yuan

ABSTRACT

The adsorption capacity and mechanism of K^+ ion onto modified-clinoptilolite (MC) for recovering potassium from seawater has been investigated in this paper. The maximum value of K^+ adsorption capacity is 36.3 mg/g (1.92 times of raw-clinoptilolite) while the modifying condition of microwave power is 450 W and heating time is 60 min. Specific surface area and pore size of absorbent has also been advanced with employing microwave. The kinetic data followed the pseudo-second-order model kinetic model, and the equilibrium data were well fitted to the Langmuir model, showing monolayer coverage of K^+ ions on the surface pores of MC. Thermodynamic parameters, including Gibbs free energy (ΔG), enthalpy changes (ΔH), and entropy changes (ΔS) were also calculated. The results demonstrated that K^+ ion was absorbed onto MC spontaneously and exothermically in nature. Thus, MC could be employed as efficient and suitable adsorbent for recovering potassium from seawater.

Key words | adsorption amount, isotherm, kinetics, modified-clinoptilolite, potassium, thermodynamic parameters

Hao Guo (corresponding author)
Chang-Sheng Peng
He-Tao Yuan
Key Laboratory of Marine Environment and
   Ecology, Ministry of Education, College of
   Environmental Science and Engineering,
Ocean University of China,
Qingdao 266100, China
E-mail: *guohao8432@126.com*

Hao Guo
Jian-Yun Jiang
Beijing Institute of High-tech Environmental
   Science,
Beijing 101111, China

Chang-Jiang Kou
CSD (Beijing) Environmental Protection
   Development Co., Ltd,
Beijing 100192, China

Jian-Yun Jiang
Fan Zhang
Beijing Association of Sustainable Development,
Beijing 100084, China

INTRODUCTION

Potassium is an important resource for agricultural production. However, the potassium resource on land is very limited, therefore recovering potassium from seawater has great prospects (Yuan *et al.* 2012). The total reserve of potassium in seawater is about 500 trillion tons (Shahmansouri *et al.* 2015). This amount is approximately 30 thousand times that of the land reserve, however the K^+ ion concentration in seawater is only 399 mg/L, and coexists with more than 80 kinds of chemical elements. The technologies of extracting potassium from seawater using zeolite as adsorbent have gained a great deal of public attention. At

present, using raw-clinoptilolite (RC) as adsorbent has been put into industrial operation (Jin *et al.* 2014). However, the K^+ ion adsorption capacity from seawater is only 14–20 mg/g due to the low purity and disproportionate quality of RC (Yuan *et al.* 2006). In order to enhance the K^+ ion adsorption capacity of RC, many modification experiments were carried out. After modifying, the characteristics of porosity and surface activity have been obviously improved.

The molecular structure of clinoptilolite consists of frameworks elements and exchangeable ions. The modification of clinoptilolite principally relates to replacement of non-skeleton and framework elements. The replacement of non-skeleton elements aimed at replacing the exchangeable ions of clinoptilolite, such as sodium, potassium, calcium and magnesium cations. Peng *et al.* (2001) used thermal sodium chloride solution soaked zeolites, the internal

holes were developed and then the specific surface area was increased. Ćurković *et al.* (1997) used 2.0 mol/L sodium chloride solution soaked zeolites at 22 and 70 °C respectively, the heavy metals removal efficiency was enhanced distinctly. Wang *et al.* (2002) used ammonium bicarbonate soaked clinoptilolite, the performance of K^+, Rb^+ and Cs^+ ion adsorption capacity was improved obviously. The replacement of framework elements aimed at replacing the aluminum ion of clinoptilolite with a hydrothermal process, and the adsorption capacity to polar molecules and ions increased with the SiO_2/Al_2O_3 ratio of molecular composition decreasing (Chang *et al.* 1984). Yang & Xu (1996) used sodium aluminate soaked zeolite β in order to supplement aluminum atoms on zeolite molecules, and characterized the samples with X-ray diffraction and nuclear magnetic resonance. Xie *et al.* (2002) also used sodium aluminate soaked zeolite β and compared catalytic activity of the samples before and after modifying, since the adsorption capacity of zeolites mainly depends on the degree of aluminum atoms replacing silicon atoms. For this reason, the replacement of framework elements is the fundamental method to modify zeolites and researched extensively (Tang & Chen 2009).

A microwave radiation heating method is capable of generating equivalent thermal effects simultaneously at different depths of absorbent inner holes (Liu *et al.* 2006). In addition, the profound heating effect was quicker and more even in contrast to the hydrothermal method, which is extensively employed in the absorbent modification, which can improve the molecular structure and advance the adsorption capacity (Liu *et al.* 2012). The organic matters in the absorbent inner holes were decomposed thoroughly with microwave heating. Consequently, the inner holes were dredged and the outside of the absorbent particles were cleaned (Zhang *et al.* 2009). With adopting microwave modification instead of a hydrothermal method, the heating time and modification effects were improved greatly (Tang & Chen 2009). The purpose of the present research was to make use of microwave modifying RC to enhance the K^+ ion adsorption amount. The effect of microwave power and heating time on adsorption amount was investigated. Then the modified-clinoptilolite (MC) was used as adsorbent to recover potassium from seawater.

Recovering potassium from seawater is a physicochemical process that involves mass transfer of a solute from liquid phase to the adsorbent surface (Hao *et al.* 2015). Adsorption kinetics were performed to assess the uptake rates and contact times needed for completion of adsorption reactions in treatment systems. Pseudo-first-order, pseudo-second-order and Weber–Morris models were normally used to study the adsorption kinetics (Wang 2016). To understand the mechanisms of adsorption, Langmuir and Freundlich models were generally used to describe the adsorption isotherms (Liu *et al.* 2016). The Langmuir isotherm assumes that the surface of the solid is homogeneous and one specific site within the adsorbent can only match a molecule without access to others, that is, the form of adsorption is monolayer. However, the Freundlich isotherm describes the process of multilayer adsorption on uneven solid surfaces (Li *et al.* 2016). In this research, the equilibrium data of using MC to recover potassium have been fitted by different kinetics and isotherm models. The thermodynamic parameters of entire adsorption process were also calculated.

MATERIALS AND METHODS

Instruments and reagents

The particle size of RC was 0.5–1.0 mm and was purchased from Jinyun County, China. Analytical-grade KCl, NaOH and $Al(OH)_3$ were purchased from Shanghai Sinopharm Chemical Reagent Co. Ltd, Shanghai. The microwave digestion furnace (JK-MDA-23, Shanghai JKI) was used to treat MC. The atomic adsorption spectroscopy (AAS, TAS-990, Purkinje general instrument) measured the concentration of K^+ ion in seawater and solution. The constant temperature vibrator (THZ-D, China Taicang Instruments, China) was employed in adsorption kinetics and isotherm experiments. The specific surface area and pore size was measured by a surface area and pore size analyzer (Autosorb-1, Quantachrome Instruments, USA). The pH at the zero point of charge (pH_{ZPC}) was determined by Zeta potential analyzer (Zetasizer Nano ZS90, Malvern Instruments, UK).

Preparation of modified clinoptilolite

MC was prepared from 1.0 g KCl and 2.0 g NaOH dissolved in 25 mL deionized water and stirred until well mixed. Then,

1.0 g Al(OH)$_3$ was added to the above mixture and stirred continuously to room temperature (20 °C). After that, 5.0 g RC was added to the mixture which was then continually stirred for 2 hours. The above mixture was heated by the microwave digestion furnace using microwave power of 75, 150, 225, 300, 375, 450, 525, 600, 675 and 750 W, and heating times of 10, 20, 30, 40, 50, 60, 70, 80, 90, 100 min; the MC was separated from the hydrothermal mixture, thoroughly rinsed with deionized water and dried in an evaporating dish. Finally, the MC was calcined for 2 hours at 400 °C in a crucible.

In a beaker, 1.0 g of MC was added to 100 mL seawater (Bohai Bay, China) then it was stirred at room temperature for 30 min. After solid phase and liquid phase were separated, the concentration of K$^+$ ion in the liquid phase was measured by AAS, and then the liquid phase was abandoned and fresh seawater was added into the solid phase for the next adsorption process. This operation was repeated three times after adsorption saturation. The K$^+$ ion adsorption amounts of MC in different modifying conditions were calculated as follows:

$$q_e = \frac{[(C_0 - C_1) + (C_0 - C_2) + (C_0 - C_3)] \times V}{m} \quad (1)$$

where q_e is the K$^+$ ion adsorption amount (mg/g) of MC at equilibrium; C_0 is the concentration of K$^+$ ion (399 mg/L) in seawater; C_1, C_2 and C_3 represent the residual concentrations (mg/L) of K$^+$ ion after the first, second and third adsorption process respectively; V and m are the volume (L) of seawater and dosages (g) of MC.

Adsorption kinetics

One gram of MC was added to 100 mL seawater and blended evenly. The concentration of K$^+$ ion (C_0) in the seawater was 399 mg/L. At 20 °C, the mixture was oscillated in a constant temperature vibrator at 120 rpm. The concentration of K$^+$ ion (C_t) in supernatant was measured by AAS at different times (20, 40, 60, 80, 100, 200, 400 and 600 min). The adsorption amounts of K$^+$ ion (q_t) were calculated based on the K$^+$ ion mass conservation. The adsorption kinetics was respectively fitted by pseudo-first-order, pseudo-second-order and Weber–Morris models.

Adsorption isotherm and thermodynamic calculating

One gram of MC was added to 100 mL KCl solution with different initial concentrations of K$^+$ ion (0.01, 0.02, 0.03, 0.04, 0.05, 0.06, 0.07 and 0.08 mol/L). The K$^+$ ion was adsorbed by MC in constant temperature vibrator at 120 rpm lasting 80 min. The concentration of K$^+$ ion in supernatant (C_e) was measured by AAS, and the equilibrium concentration of K$^+$ ion onto MC (q_e) was calculated based on the K$^+$ ion mass conservation. The adsorption isotherm was measured at different temperatures (283, 293, 313 and 333 K) and fitted by Langmuir and Freundlich isotherm models respectively. Finally, the thermodynamic parameters such as ΔG^0, ΔH^0 and ΔS^0 were calculated.

RESULTS AND DISCUSSION

Effect of pH value to adsorption amount

The K$^+$ ion adsorption amount with different pH values is shown in Figure 1. The results indicate that the maximum K$^+$ ion adsorption amount onto MC is at pH 6.0–8.0. The K$^+$ ion adsorption amount was severely influenced in acidic conditions when the concentration of KCl solution was 0.001 mol/L. However, the K$^+$ ion adsorption amount was barely influenced by the change of pH value when the concentration of KCl solution was 0.01 and 0.1 mol/L. Consequently, neutral conditions were chosen to carry out the adsorption reactions. In addition, the pH value of seawater was impossibly adjusted in the case where the MC was employed in the engineering due to economy and the complexity of the seawater, because the treatment scale of seawater is enormous and most plants cannot afford the high requirements of acid or alkali.

Effect of microwave power and heating time

Figure 2 shows the K$^+$ ion adsorption amount of MC with different microwave power and heating time modifying conditions. It is evident that the maximum value of the K$^+$ ion adsorption amount is 36.3 mg/g, with microwave power of 450 W and heating time of 60 min. It also can be observed
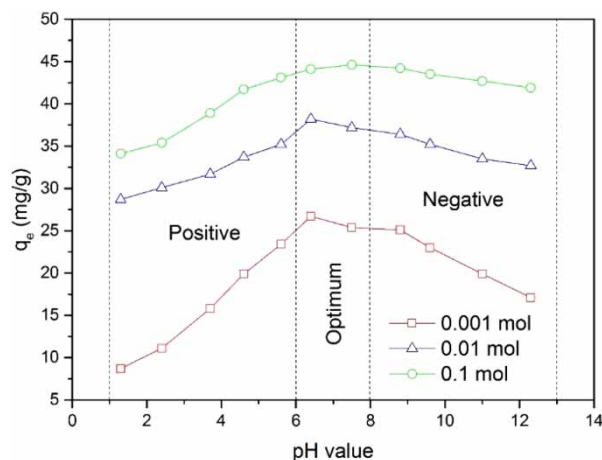
Figure 1 │ K⁺ ion adsorption amount with different pH values of the solution.

that when the microwave power and heating time was greater or less than 450 W and 60 min, the K⁺ ion adsorption amount curve declined quickly. This is because when using lower microwave power and less heating time, the soaking solution temperature is also lower. This will affect the aluminum-silicon replacing velocity and exchange extent. However, using higher microwave power and longer heating time, the soaking solution temperature raised quickly and the solution was boiling, the solid–liquid ratio of reaction system was changed and the internal water of MC escaped. The structure of the MC molecule was destroyed and the conversion ratio declined with elapsing time (Querol *et al.* 1997).

Adsorption capacity of RC and MC

As shown in Figure 3, the potassium adsorption capacity of RC and MC is 18.9 and 36.3 mg/g respectively. With microwave modification, the increment of adsorption capacity reached 92%. Consequently, the adsorption capacity of potassium by MC was significantly improved from the results.

Adsorption kinetics

In order to understand the transfer mechanism of K⁺ ion from liquid phase to solid phase, three adsorption kinetics models were used to describe the K⁺ ion transfer process from seawater onto MC. The linear form of pseudo-first-order kinetic model is shown in the following equation (Hao *et al.* 2015):

$$\ln(q_e - q_t) = \ln q_e - k_1 t \qquad (2)$$

where q_e (mg/g) is the adsorption amount of K⁺ ion at equilibrium (36.3 mg/g), q_t is the adsorption amount of K⁺ ion at time t (*min*), k_1 (1/min) is the rate constant of the pseudo-first-order kinetic model.

The linear form of the pseudo-second-order kinetic model is expressed by Equation (3):
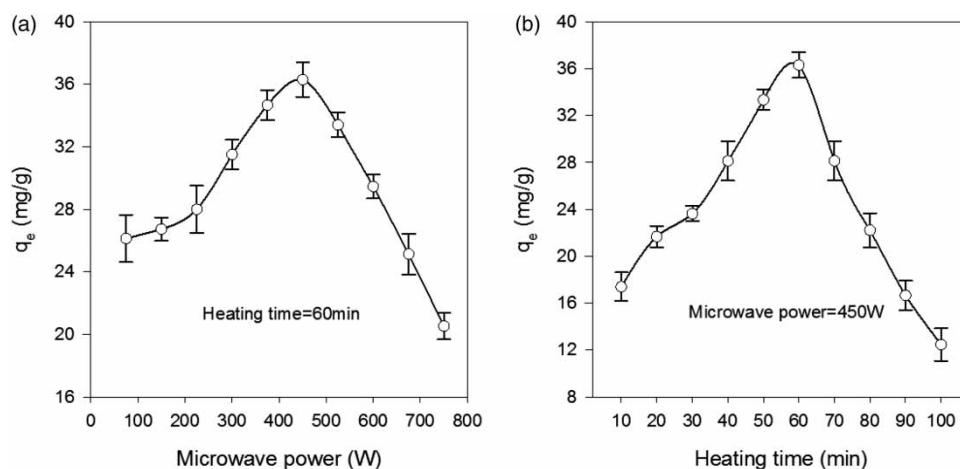
$$\frac{t}{q_t} = \frac{t}{q_e} + \frac{1}{h} \qquad (3)$$

Figure 2 │ K⁺ ion adsorption amount with (a) different microwave power and (b) heating time modifying conditions.
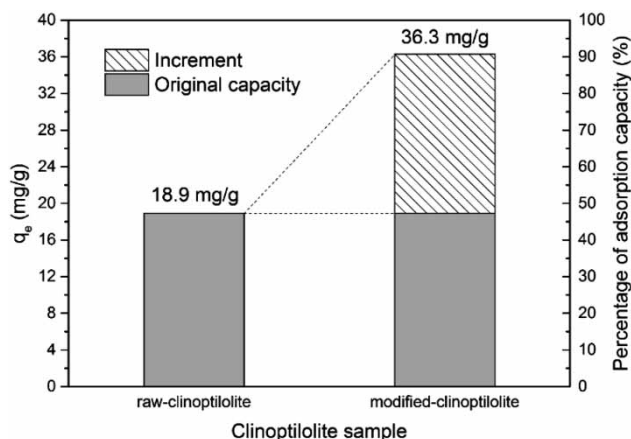
Figure 3 | Comparison of potassium adsorption capacity between RC and MC.

Moreover, the initial adsorption rate h when $t = 0$ is defined in the following equation (Cardoso *et al.* 2004):

$$h = k_2 q_e^2 \tag{4}$$

where k_2 (g/(mg · min)) is the rate constant of pseudo-second-order kinetic model, and the intercept of Equation (3) was applied to calculate the k_2 value.

In accordance with the Weber–Morris model, the intra-particle diffusion stage controls the adsorption rate and the stage from liquid to adsorbent surface can be neglected. The model is expressed by the following Equation (5) (Tsai *et al.* 2005):

$$q_t = k_p t^{1/2} + C \tag{5}$$

where k_p (g/(mg · min)) is the rate constant of Weber–Morris, C value is the intercept of this plot. If the intra-particle diffusion stage is the rate-limiting step, the plot of q_t against $t^{1/2}$ should go through the origin, the value of which is equal to zero.

On the basis of equilibrium data of the K$^+$ ion adsorption amount, Figure 4 shows the effect of different times on the adsorption amounts of K$^+$ ion onto MC in (a) seawater, (b) linear fit of pseudo-first-order, (c) pseudo-second-order and (d) Weber–Morris models. As can be seen from Figure 2(a), the overall trend was an increase in adsorption amount with elapsing time. It was observed that the K$^+$ adsorption rate was rapid from the beginning of the experiment and before 80 min, thereafter it proceeded with a slower rate and finally reached saturation.

The linear fit parameters of three kinetics models are listed in Table 1. Judging from the R^2 value, we can see that the pseudo-second-order in Figure 4(c) gives the best fitting result for all cases. This suggests that the K$^+$ ion adsorption process should mainly be involving exchange or sharing of electrons between K$^+$ cations and functional groups. In addition, the linear fit of Weber–Morris Figure 4(d) models can be classified into two phases, also showing that intra-particle diffusion is not the only rate-limiting step in the adsorption process.

Adsorption isotherm

To clarify the adsorption mechanism of K$^+$ ion onto MC, two commonly used types of isotherm models, Langmuir and Freundlich, were applied to explain the K$^+$ ion adsorption process (Kumar 2007). The Langmuir model assumes that the process of monolayer adsorption on a homogeneous solid surface, where one specific site within the adsorbent can only match a molecule without access of others and the model is given by the following linear equation:

$$\frac{C_e}{q_e} = \frac{1}{b q_m} + \frac{C_e}{q_m} \tag{6}$$

where q_e (mg/g) is the adsorption amount of K$^+$ ion onto MC surface at equilibrium and C_e (mg/L) is the concentration of KCl solution at equilibrium, q_m (mg/g) and b (L/mg) are the amount of maximum adsorption amount and Langmuir constant, respectively.

Moreover, R_L value reflects the tendency of the adsorption process, when the value of R_L is between 0 and 1, it indicates the adsorption process is favorable, otherwise, it is unfavorable. The R_L value can be inferred as follows:

$$R_L = \frac{1}{1 + b C_0} \tag{7}$$

The Freundlich model is an empirical model, describing the process of multilayer adsorption on an uneven solid surface. The Freundlich linear model is expressed by the following equation (Li *et al.* 2016):

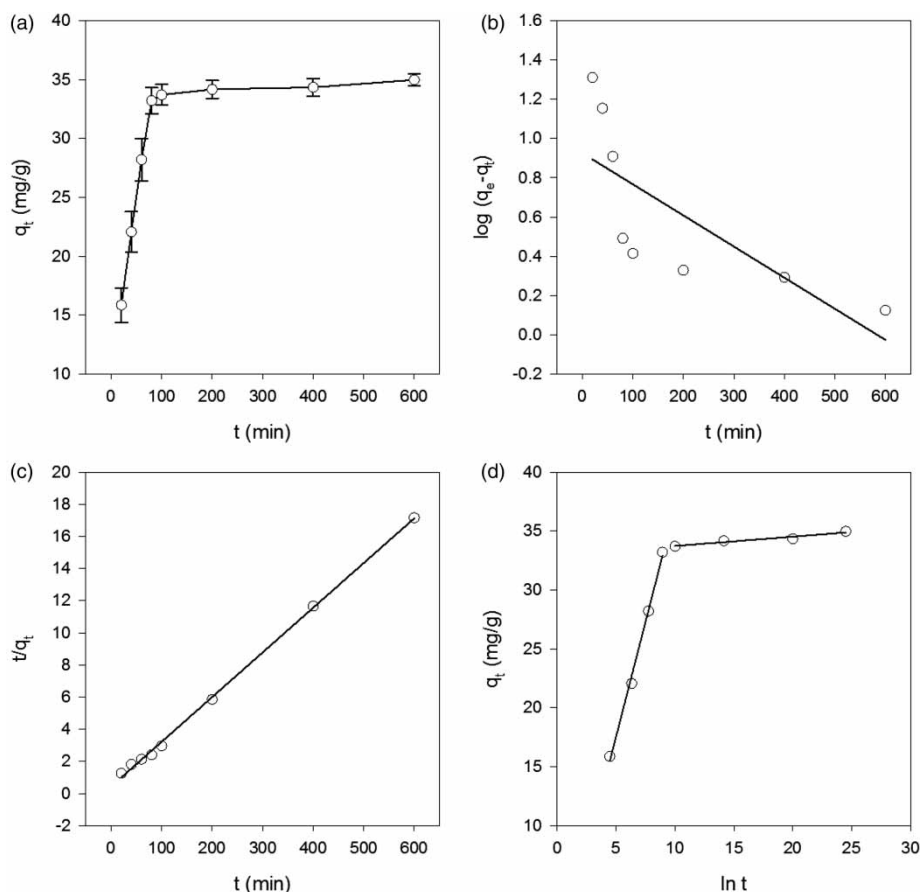$$\log q_e = \log K_f + \frac{1}{n} \log C_e \tag{8}$$

Figure 4 │ Effect of different times on the K$^+$ ion adsorption amounts onto MC in (a) seawater, (b) linear fit of pseudo-first-order, (c) pseudo-second-order and (d) Weber–Morris models.

Table 1 │ Parameters of linear fit of pseudo-first-order, pseudo-second-order and Weber–Morris models

							Weber–Morris			
Kinetic models	Pseudo-first-order			Pseudo-second-order			1st stage		2nd stage	
Parameters	$k_1 \times 10^3$	q_e	R^2	$k_2 \times 10^3$	q_e	R^2	C	R^2	C	R^2
Values	2.00	2.52	0.564	1.77	35.71	0.999	−1.94	0.996	32.93	0.932

where q_e (mg/g) and C_e (mg/L) represent the adsorption amount of K$^+$ ion onto MC and K$^+$ ion concentration of KCl solution at equilibrium, K_f and n are the constant of the model, expressing the adsorption amount and the intensity of the adsorption process. In addition, $1/n$ reflects the tendency of the adsorption process, when the value of $1/n$ is between 0.1 and 0.5, this indicates that the adsorption process is favorable, if the $1/n$ value is greater than 2, the adsorption process becomes difficult (Li *et al.* 2016).

On the basis of equilibrium data of K$^+$ ion adsorption amount onto MC, Figure 5 shows the linear fit of (a) the Langmuir model and (b) the Freundlich model at different temperatures (283, 293, 313 and 333 K).

The parameters of two isotherm models are listed in Table 2. Because the R^2 values of the Langmuir model are closer to 1 than the Freundlich model, it can be deduced that the Langmuir model fits the equilibrium data better than the Freundlich model. Therefore, the Langmuir
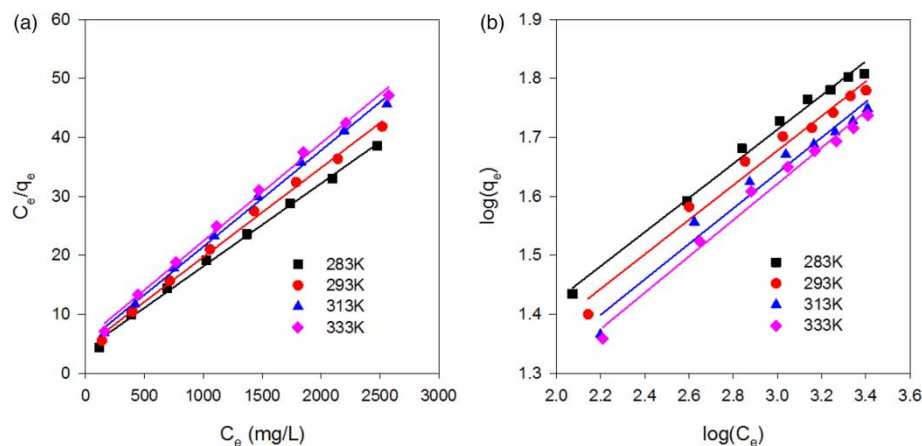
Figure 5 │ Linear fit of (a) the Langmuir model and (b) the Freundlich model.

Table 2 │ Parameters of the Langmuir and Freundlich equations

Temperature (K)	Langmuir model				Freundlich model		
	q_m (mg/g)	b	R^2	R_L	K_f	$\frac{1}{n}$	R^2
283	71.43	0.0035	0.996	0.08–0.42	7.00	0.290	0.991
293	66.67	0.0033	0.996	0.09–0.44	6.30	0.293	0.978
313	62.50	0.0031	0.997	0.09–0.45	5.47	0.301	0.969
333	58.82	0.0029	0.996	0.10–0.47	4.99	0.308	0.985

model is in better accordance with the process of K$^+$ ion adsorption. In addition, the R_L values of the Langmuir model are between 0 and 1, and the $1/n$ values of the Freundlich equation are between 0 and 0.5, indicating that the adsorption process is favorable. The range of q_m is between 58.82 and 71.43 mg/g, and the maximum q_m occurs at 283 K, it is also shown that the value of q_m increases with decreasing temperature. This feature corresponds with physisorption characteristics because the lower temperature could promote the rate of physisorption process.

Thermodynamic parameters

The data obtained from the temperature study were used for thermodynamic analysis. Thermodynamic analysis focused on Gibbs free energy (ΔG), which can also be expressed using enthalpy changes (ΔH) and entropy changes (ΔS). These parameters imply the feasibility of the adsorption process and are obtained using Equations (9)–(11) (Gupta *et al.* 2012):

$$\ln K_L = \frac{\Delta S}{R} - \frac{\Delta H}{RT} \tag{9}$$

$$K_L = M_{K^+} \times 55.6b \tag{10}$$

$$\Delta G = \Delta H - T\Delta S \tag{11}$$

where K_L (L/g) represents the Langmuir constant, R (J/(mol · K)) is the universal gas constant, 8.314 J/(mol·K), ΔS (J/(mol · K)) and ΔH (kJ/mol) were calculated from the slope and intercept of $\ln K_L$ against $1/T$ plot as shown in Figure 6, ΔG (kJ/mol) values with different temperatures were calculated from Equation (11), M_{K^+} (g/mol) is the atomic mass of potassium.

The calculated thermodynamic parameters are listed in Table 3. Negative ΔG and ΔH indicates that the adsorption of K$^+$ ion onto MC was an exothermic reaction. A positive value of ΔS suggests that an increased randomness occurs at the solid solution interface in the internal structure. The ΔG value obtained was relatively low (<20 kJ/mol),
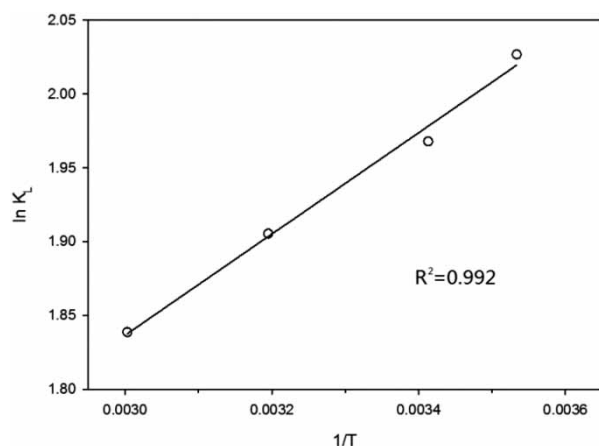
Figure 6 | Plot of $\ln K_L$ against $1/T$ for calculation of thermodynamic parameters.

Table 3 | Thermodynamic parameters for the adsorption of K^+ ion onto MC

Temperature (K)	K_L (L/g)	ΔG (kJ/mol)	ΔH (kJ/mol)	ΔS (J/(mol·K))
283	7.589	–4.751	–2.850	6.719
293	7.156	–4.819		
313	6.722	–4.953		
333	6.288	–5.087		

Table 4 | Characteristics of specific surface area and pore size between RC and MC

Zeotypes	Specific surface area (m²/g)	External surface area (m²/g)	Micro-pore area (m²/g)	Micro-pore volume (cm³/g)	Average pore size (Å)
RC	121.90	16.15	105.75	0.064	38.18
MC	140.50	13.30	127.20	0.074	39.13

suggesting that the adsorption process follows a physisorption mechanism (Hameed *et al.* 2007). Furthermore, the decrease in the values of ΔG with increasing temperature

revealed the adsorption was naturally more spontaneous at lower temperatures (Liu *et al.* 2012).

Surface characteristics and pH$_{ZPC}$ of RC and MC

The surface characteristics of adsorbent significantly affected the adsorption capacity. The specific surface area and pore size was measured by a surface area and pore size analyzer. The properties comparison between RC and MC are compared in Table 4. The results indicate that the specific surface area (including external surface area and micro-pore area) was increased after microwave modification. However, the average pore of MC was slightly increased. Consequently, the adsorption capacity of potassium was increased with the specific surface area increasing.

Chemical properties of the adsorbent were also rather important for adsorption. The pH at the zero point of charge (pH$_{ZPC}$) was determined by a Zeta potential analyzer, 0.25 mol/L HCl and 0.25 mol/L NaOH were prepared to adjust the pH value of the KCl solution to 2, 3, 4, 5, 6, 7 and 8. As shown in Figure 7(a) and 7(b), the plots of Zeta potential against pH indicated that the pH$_{ZPC}$ of RC and MC was 5.1 and 4.3, respectively.

CONCLUSIONS

The present work shows that the K^+ ion adsorption capacity of MC reached 36.3 mg/g (1.92 times of RC) when recovering potassium from seawater. The optimum modification conditions of microwave power and heating time for modifying clinoptilolite are 450 W and 60 min respectively. On account of employing microwaves to promote the modifying
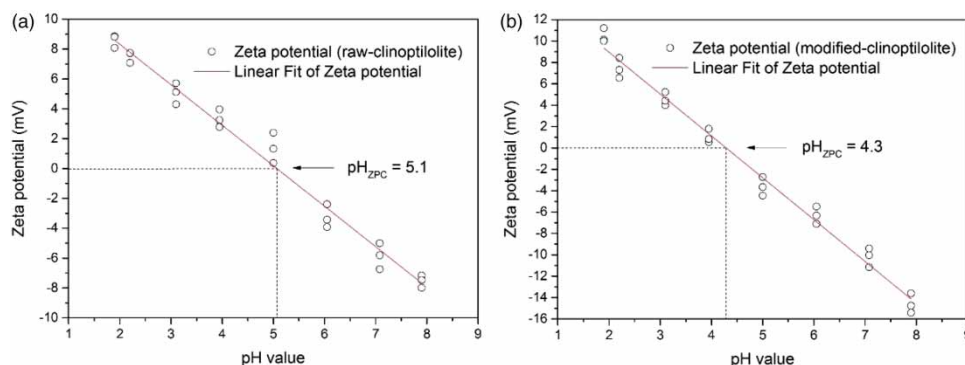

Figure 7 | Zeta potential of (a) RC and (b) MC at different pH values.

process, the specific surface area and pore size of absorbent has also been advanced. The adsorption kinetics follows the pseudo-second-order model, and the equilibrium data were well fitted to the Langmuir model, showing monolayer coverage of K^+ ion onto the surface pores of MC. Thermodynamic parameters, including Gibbs free energy (ΔG), enthalpy changes (ΔH), and entropy changes (ΔS), were also calculated. The results demonstrated that K^+ ion was naturally absorbed onto MC spontaneously and exothermically. Thus, the MC is applicable for recovering potassium from seawater as adsorbent.

ACKNOWLEDGEMENTS

REFERENCES

Cardoso, V. D. A., Souza, A. G. D., Sartoratto, P. P. C. & Nunes, L. M. 2004 The ionic exchange process of cobalt, nickel and copper(II) in alkaline and acid-layered titanates. *Colloids Surf. A* **248**, 145–149.

Chang, C. D., Chu, C. T.-W., Miale, J. N., Bridge, R. F. & Calvert, R. B. 1984 Aluminum insertion into high silica zeolite frameworks. 1. Reaction with aluminum halides. *J. Am. Chem. Soc.* **106**, 8143–8146.

Ćurković, L., Cerjan-Stefanović, Š. & Filipan, T. 1997 Metal ion exchange by natural and modified zeolites. *Water Res.* **31** (6), 1379–1382.

Gupta, V. K., Pathania, D., Agarwal, S. & Sharma, S. 2012 De-coloration of hazardous dye from water system using chemically modified *Ficus carica* adsorbent. *J. Mol. Liq.* **174**, 86–94.

Hameed, B. H., Ahmad, A. A. & Aziz, N. 2007 Isotherms, kinetics and thermodynamics of acid dye adsorption on activated palm ash. *Chem. Eng. J.* **133**, 195–203.

Hao, H., Feng, J. G., Chen, W. T., Xiang, S., Liu, W. J. & Wu, X. M. 2015 Adsorption behavior of herbicide paraquat from aqueous solutions using starfish particles: kinetic, isotherm, and thermodynamic studies. *Asia-Pac. J. Chem. Eng.* **10**, 347–355.

Jin, N., Meng, C. X. & Hou, J. 2014 Preparation and characterization of merlinoite for potassium extraction from seawater. *J. Ind. Eng. Chem.* **20**, 1227–1230.

Kumar, K. V. 2007 Optimum sorption isotherm by linear and non-linear methods for malachite green onto lemon peel. *J. Dyes Pigm.* **74**, 595–597.

Li, D. D., Li, J. Q., Gu, Q. B., Song, S. X. & Peng, C. S. 2016 Co-influence of pore size of adsorbents and the structure of adsorbates on adsorption of dyes. *Desalin. Water Treat.* **57** (31), 14686–14695.

Liu, J. H., Lv, X. L., Wei, L. D., Cheng, Z. Q., Zhang, N. L. & Dou, S. 2006 Study on adsorbing sulfide of diatomite modified by microwave and vitriol. *Non-Metal. Mine.* **29** (3), 36–37.

Liu, F., Chung, S., Oh, G. & Seo, T. S. 2012 Three-dimensional grapheme oxide nanostructure for fast and efficient water-soluble dye removal. *ACS Appl. Mater. Inter.* **4**, 922–927.

Liu, X. Y., Wang, B. Y. & Su, Z. X. 2016 Enhanced adsorptive removal of methylene blue from aqueous solution by soft rush (Juncus effusus). *Desalin. Water Treat.* **57** (4), 1671–1683.

Peng, C. S., Meng, H. & Song, C. Y. 2001 Studies on characteristics of activated zeolite in the further treatment of light polluted water. *Non-Metal. Mine.* **23** (3), 48–49.

Querol, X., Alastuey, A., López-Soler, A., Plana, F., Andrés, J. M., Juan, R., Ferrer, P. & Ruiz, C. R. 1997 A fast method for recycling fly ash: microwave assisted zeolite synthesis. *J. Environ. Sci. Technol.* **31** (9), 2527–2533.

Shahmansouri, A., Min, J., Jin, L. Y. & Bellona, C. 2015 Feasibility of extracting valuable minerals from desalination concentrate: a comprehensive literature review. *J. Clean. Prod.* **100**, 4–16.

Tang, Q. & Chen, N. C. 2009 Progress in research on natural zeolite modified methods. *Mater. Rev.* **23** (S1), 439–441.

Tsai, W. T., Chang, Y. M., Lai, C. W. & Lo, C. C. 2005 Adsorption of basic dyes in aqueous solution by clay adsorbent from regenerated bleaching earth. *Appl. Clay Sci.* **29**, 149–154.

Wang, B. Y. 2016 Enhancement of metal bioleaching from sewage sludge by cotton stalk. *Desalin. Water Treat.* **57** (4), 1713–1721.

Wang, X. J., Gao, S. Y., Zhou, J. G. & Lu, Y. 2002 Study on the extraction and separation of K^+, Rb^+, Cs^+ with natural clinoptilolite from geothermal water in Tibet. *J. Salt Lake Res.* **10**, 31–37.

Xie, Z. K., Bao, J. Q., Yang, Y. Q., Chen, Q. L. & Zhang, C. F. 2002 Effect of treatment with $NaAlO_2$ solution on the surface acid properties of zeolite β. *J. Catal.* **205**, 58–66.

Yang, C. & Xu, Q. H. 1996 Alumination of zeolite β. *Acta. Phys-Chim. Sin.* **12** (12), 1057–1060.

Yuan, J. S., Guo, Z. S. & Zhang, L. D. 2006 Characterization of new type molecular sieve for potassium and its exchange capability to K^+. *Chin. J. Process. Eng.* **6** (6), 903–906.

Yuan, J. S., Zhao, Y. Y., Li, Q. H., Ji, Z. Y. & Guo, X. F. 2012 Preparation of potassium ionic sieve membrane and its application on extracting potash from seawater. *Sep. Purif. Technol.* **99**, 55–60.

Zhang, Y. J., Chen, L., Ma, J., Zhang, L., Yao, J. & Wu, P. Y. 2009 Study on ammonia nitrogen removal using modified zeolites by microwave. *Chin. Water Wastewater* **25** (1), 72–74.